

Cosmic Ray, Beam-Halo and Beam-Gas Rate Studies for ATLAS Commissioning

M.Boonekamp^a, F.Gianotti^b, R.A.McPherson^c, M.Nessi^b and P.Nevksi^d

^a CEA, DSM/DAPNIA, Centre d'Etudes de Saclay, F-91191 Gif-sur-Yvette, France.

^b CERN, European Organisation for Nuclear Research, CH-1211 Geneva 23, Switzerland.

^c University of Victoria, Department of Physics, P O Box 3055, Victoria BC V8W 3P6, Canada and Fellow of the Canadian Institute of Particle Physics.

^d Brookhaven National Laboratory (BNL), Upton New York.

Abstract

Prior to LHC beam-beam collisions, the first exposure of ATLAS to high-energy particles from cosmic rays, and also beam-halo and beam-gas events during single beam running, can be used for detector commissioning. The barrel calorimeter system should be able to take cosmic events already in 2005, and increasingly more sub-detectors will be installed and commissioned over the following two years. In late 2006 and early 2007, significant samples of cosmic ray events can be collected with the full ATLAS detector in place. In spring 2007, three months of LHC single-beam running are planned, which can be used to accumulate both beam-halo and beam-gas events for detector studies. Efficient use of these commissioning periods and data samples will prepare ATLAS for the first beam-beam collisions, expected in mid-2007.

In this note, we present the first full simulation studies of the expected fluxes from cosmic ray muons, beam-halo muons and beam-gas events for the ATLAS commissioning period.



1 Introduction

Commissioning ATLAS will be a major enterprise. Past experience with smaller and simpler detectors tells us that bringing an experiment from the end of the installation to the ready-to-take-good-data stage is a difficult and painful task, which usually takes more time than foreseen. An efficient, timely and well organized commissioning programme, where one tries to understand and fix as much as possible as early as possible, is therefore crucial to reach quickly this stage at the LHC.

The ATLAS commissioning plan prepared by the Technical Coordination is sketched in Fig. 1. It is divided into four phases. The first three cover mainly the commissioning at the sub-detector level, based on hardware tools (e.g. electronic calibration). Phase D, which starts at the end of 2006, addresses the commissioning of the whole detector using “physics data”, and can in turn be divided into four phases:

- Phase 1: Cosmics run. This period will start at the end of 2006 and will extend over the first three months of 2007, during the machine cool-down. In this case the “physics data” are cosmic muons. It should be noted that for some sub-detectors, namely the calorimeters, cosmics runs can start earlier, since these detectors will be installed and equipped with electronics and local DAQ systems already in 2005.
- Phase 2: Single-beam period. According to the present machine planning [1], the cool-down period will be followed by a period of about two months in which the machine will be commissioned mainly with a single beam. This is expected to happen approximately in April-May 2007. The only “physics data” that the experiments can hope to collect in this phase, in addition to cosmic muons, are beam-halo muons and beam-gas interactions.
- Phase 3: First pp collisions. In this phase, the main and most urgent task will be to understand the trigger and the detector with the first real events from the Collider. A major step will be to set up the trigger in as an unbiased way as possible (by using mainly minimum-bias events at the beginning). Minimum-bias and QCD di-jet events, as well as clean physics samples like $Z \rightarrow \ell\ell$ and $t\bar{t}$ events, will be used also to calibrate the detector and understand the main performance issues (b -tagging, absolute energy scale, etc.).
- Phase 4: Physics commissioning. In this period, in addition to continuing the detector commissioning, the main goal will be to understand basic standard physics processes at 14 TeV (e.g. W/Z production, top physics), and in particular measure the backgrounds to possible discovery channels.

Studies have started in the physics community in February 2003, with the aim of understanding what we can learn during each one of the above phases. Examples of the questions which have been (and are) addressed are the following. For Phases 1 and 2, are the rates of cosmic muons, beam-halo muons and beam-gas interactions large enough for ATLAS commissioning studies? Do we have the trigger for these atypical events? Can we hope to calibrate and align the detector with these data, or are they only useful for basic debugging, like the mapping of dead channels? In Phase 3 one major question is what is the strategy to commission the trigger in as an unbiased way as possible; also, what is the expected detector performance at this stage and what are the strategy and data samples needed to bring the detector up to the level required to perform first sensible physics studies? Finally, in Phase 4 the questions are physics-oriented: what is the expected precision of early measurements of the basic Standard Model physics processes? How well do we need to determine the backgrounds to the various new physics channels in order to extract a convincing signal as soon as possible, and what is the strategy to achieve this goal?

First results have been reported at the Athens Physics Workshop [2], at the Prague Commissioning Workshop [3], and in a series of dedicated meetings [4].

The purpose of this note is to present the expected rates of cosmic muons, beam-halo muons and beam-gas events, as well as the energy spectra of the involved particles, as a first step for a better understanding of the utility of Phases 1 and 2, and as an input to the sub-detector communities. It should be noted that these three samples are quite complementary. Cosmic muons illuminate mainly the barrel part of the detector, whereas beam-halo muons are important mainly for the end-caps. Finally, beam-gas interactions are potentially very useful for the tracking system but of little relevance for the calorimeters and the muon spectrometer. The results presented here have been obtained with full and detailed GEANT3 simulations of the ATLAS detector.

Some very preliminary thoughts about possible trigger schemes for these events are also mentioned, and some examples of questions and studies to be addressed in the near future are given.

2 Detector Simulation

These studies have been done using GEANT3-based detector simulations of the initial staged layout of the experiment in 2007. In addition to the standard ATLAS simulation geometry, the beam shielding materials, important for the single beam commissioning simulations, have been introduced according to the latest layout proposed by the Radiation Task Force in January 03 [5]. The detailed geometry description spans up to ± 23 m from the interaction point along the beam axis, i.e. up to the beginning of the cavern concrete wall.

The simulation also includes the cavern overburden, the layout of the access shafts and to some approximation the material of the surface buildings. The density of the overburden was taken to be equal 2.33 g/cm^3 (the engineering data varies from 2.3 to 2.5 g/cm^3 as a function of depth). The simulated layout is shown in Fig. 2.

3 Event samples

3.1 Cosmic ray muons

Two cosmic ray generators have been used, both of which are single muon “guns”. The muons are simulated starting at the surface, with energy and angular distributions expected from cosmic ray muon fluxes. The few cuts which are applied to the muons at generation time in order to speed up the simulation are summarized in Table 1. Note that for the cosmic ray plots and discussion, θ is defined such that a vertical, downward-going muon has $\theta = 0$ (i.e. $\cos \theta = 1$).

The first generator uses the cosmic muon flux from an approximation formula from the Particle Data Group, labeled “PDG” in this note. The surface flux is approximated as [6]

$$\frac{dN_\mu}{dE_\mu} = \frac{0.14E_\mu^{-2.7}}{\text{cm}^2 \text{ s sr GeV}} \times \left\{ \frac{1}{1 + \frac{1.1E_\mu \cos \theta}{115 \text{ GeV}}} + \frac{0.054}{1 + \frac{1.1E_\mu \cos \theta}{850 \text{ GeV}}} \right\}, \quad (1)$$

where the two terms give the contributions from charged pion and charged kaon decays, respectively. This formula neglects muon decay-in-flight, which is negligible only for $E_\mu > 100/\cos \theta \text{ GeV}$. Typical muons which vertically traverse the rock overburden above ATLAS and pass through the complete experiment have a surface energy of at least 50 GeV, so the generator based on this formula is expected to somewhat overestimate the lower energy part of the cosmic muon flux distribution.

The second generator is based on fits to measured cosmic ray muon surface fluxes [7]. The code is based on programs provided by Alois Putzer, with some modifications to allow for robust

Location	Cut
Surface	$0.35 < \cos \theta < 1.0$ (up to 70° from vertical)
	$10 \text{ GeV} < E_\mu < 5000 \text{ GeV}$
	$-300 \text{ m} < X_0 < +300 \text{ m}$
	$-300 \text{ m} < Z_0 < +300 \text{ m}$
Extrapolation to ATLAS $Y = 0$	$-30 \text{ m} < X(Y = 0) < +30 \text{ m}$
	$-30 \text{ m} < Z(Y = 0) < +30 \text{ m}$

Table 1: *Summary of cuts used in cosmic muon Monte Carlo samples. The muons are thrown in a large area ($\pm 300 \text{ m}$) on the surface to insure that all interesting events are retained. The “extrapolation” cuts use a straight-line projection from the surface to the plane $Y = 0$ (ATLAS coordinates) and require the muon be within a $\pm 30 \text{ m}$ box. A vertical, downward-going muon is defined to have $\cos \theta = 1$.*

probability sampling for the entire energy range used in these studies. This generator is denoted “ALE” in this note. The fluxes from the generator agree with the measurements at the few percent level; however, the Particle Data Group indicates that the cosmic normalization is valid only at the 10–15% level [8], which should probably be taken as the error on all rates determined with this generator.

The Monte Carlo samples used in the studies for this note are summarized in Table 2. As expected, the PDG flux is larger than that from the ALE generator, by a factor of ~ 2 for surface muon energies of 10 GeV.

Description		PDG	ALE
Surface	rate	$6.3 \times 10^{-3} \mu/(\text{cm}^2\text{s})$	$3.0 \times 10^{-3} \mu/(\text{cm}^2\text{s})$
	Number Generated	19×10^9	19×10^9
Cavern	rate	5.9 kHz	4.9 kHz
	Number Generated	5.0×10^6	8.6×10^6
Real Time		840 sec	1747 sec

Table 2: *Summary of cosmic muon rates and samples. Cuts applied on the sample generation are described in Table 1.*

The cosmic muons were then passed through the GEANT3 simulation described in Section 2. Technically, the muons are saved when they enter the standard ATLAS GEANT3 detector volume, enabling efficient re-use of the events with different ATLAS detector configurations without repeating the time-consuming overburden simulation. The studies so far have used the so-called “initial detector”, and different configurations of the magnetic fields from the toroids and solenoid. The software tools and simulated samples are summarized at [9].

Cosmic muon rates for different subsets of the muon samples are summarized in Table 3. The rate of cosmic events with at least one hit somewhere in the ATLAS detector is about 3 kHz. The rate of “event-like” cosmic muons, defined as events that have muon trigger chamber hits on both the upper ($Y > 0$) and lower ($Y < 0$) halves of ATLAS, and also hits in the pixel detector, is about 0.7 Hz. One month of fully efficient running would thus give about 2 M “event-like” cosmic muons, which would be a very useful sample for many ATLAS commissioning studies. The expected kinematic distributions (defined when the muons enter the standard ATLAS GEANT3 detector volume) are shown in Figs. 3 and 4 for muons with at least one detector hit, and in Figs. 5 and 6 for “event-like” muons.

Description		Rates (Hz)	
		PDG	ALE
Enter ATLAS cavern		5900	4900
≥ 1 detector hit		4100	3400
Through Going	RPC top and bottom, Inner Detector hit	40	35
	RPC top and bottom, Pixel hit	0.9	0.7
Passed \sim Origin	$Z_{\text{hit}} < 300$ cm, $R_{\text{hit}} < 60$ cm	18	15
	$Z_{\text{hit}} < 60$ cm, $R_{\text{hit}} < 20$ cm	1.0	0.7
Calorimeter Energy Deposit	EM cal energy > 5 GeV	0.7	0.6
	Tile cal energy > 20 GeV	2.5	2.0

Table 3: *Summary of cosmic muon predicted rates. The ALE generator should give the better rate estimates, with a systematic error of about 10–15%.*

3.2 Cosmic muon flux measurement

To verify the predicted fluxes we have performed measurements of the cosmic muon rates in the ATLAS experimental hall using a muon telescope. The telescope consisted of two pairs of scintillator counters (about 400 cm² each) interleaved by 5 cm of lead. The telescope was moved on the floor of the ATLAS cavern along the future beam axis. Figure 7 shows a schematic layout of the muon telescope, and the telescope parameters are summarized in Table 4.

Counter	width (cm)	length (cm)	thickness (cm)
1	18	30	1.0
2	20.5	22	2.0
3	16	22	1.0
4	16	16.5	1.0

Table 4: *Dimensions of the scintillator counters used for the cosmic ray rate measurements in the ATLAS cavern.*

The rates were counted by four coincidence schemes, two close to the vertical direction and two close to a 45 degree incidence angle.

The measured vertical rates are shown in Fig. 8 as a function of the telescope position along the beam axis. The predicted rates were calculated using a GEANT3 simulation of the ATLAS hall and of the telescope, and the “ALE” generator described in Section 3.1. A good agreement is observed, giving confidence in the results reported in Section 3.1.

3.3 Beam-halo

Machine-induced secondary particles, expected as soon as the first beam circulates, potentially provide a second means of preliminary commissioning of the ATLAS detector. The halo particles cross the detector from side to side, leaving signals essentially in the end-cap regions, and are thus complementary to the cosmic ray muons discussed above.

Calculations of the beam-induced particle fluxes have been performed for the ATLAS interaction point in [10], and are briefly outlined in the following. The machine settings correspond to the LHC optics version 6.4, a β^* at the ATLAS interaction point of 0.5 m, and a circulating current of 0.54 A per beam, corresponding to the nominal high luminosity running. Results were obtained for the beam circulating clockwise, *i.e.* entering the ATLAS cavern from the LHCb side (the LHC layout is illustrated in Fig. 9).

Secondary particle fluxes in the machine are mainly due to elastic and inelastic scattering of the beam protons on the residual gas in the vacuum pipe, beam cleaning inefficiency, and

Particle species	Flux (kHz)
All	1750
Charged hadrons	1515
Neutrons	130
Muons	105

Table 5: *Total beam-halo particle flux at the scoring plane (see text), and breakdown per species.*

elastic beam-beam scattering at the high luminosity insertion regions. The vacuum quality and the residual gas compositions are taken from [11], where an average value of $3 \cdot 10^{-8}$ Torr was obtained (this number actually varies with position and is given here indicatively).

It is assumed that secondary particles produced upstream of LSS7 (see Fig. 9) are stopped at this point, where the aperture of the cleaning system is very small. Starting from there, all the particle production sources listed above are included in the simulation. Hadronic cascades originating from interactions between the beam losses and the machine elements are also simulated if they occur in the straight section preceding the ATLAS experimental area. Secondaries with a kinetic energy smaller than 20 MeV are discarded. The particles are transported (following the LHC optics and taking into account the material distribution along the beam line) up to the so-called “scoring plane”, situated after the last quadrupole triplet at 23 m from the ATLAS interaction point. The particles are counted at this plane, which corresponds to the wall of the ATLAS cavern. The total flux, as well as spatial, angular and energy distributions, are available. The total particle flux, and its breakdown in particle species, is given in Table 5. Figure 10 illustrates radial and energy distributions of muons at the ATLAS cavern entrance. The average muon energy is a few GeV, with important tails up to a few TeV. The muons are democratically distributed within a radius of about 3.5 m, thus illuminating all ATLAS sub-detectors.

Starting from these simulations, a number of assumptions were made to estimate the flux expected during the initial machine operation. It is anticipated [12] that during the single-beam period only about 50 bunches will circulate instead of the nominal 2808, and that every bunch will contain roughly 3×10^{10} protons instead of 10^{11} expected in high-luminosity running. This leads to a reduction factor of the total beam current of approximately 200, which has been taken into account in the results given below. It should be noted that that this assumption depends crucially on the details of the machine commissioning scenario, which will be refined during the coming years. Additionally, it is inconsistent to assume a smaller machine current together with the nominal vacuum¹, since part of the residual gas is actually beam-induced. A lower machine current could thus imply a somewhat better vacuum and further reduction of the beam-halo rates.

Beyond the scoring plane, the ATLAS simulation framework takes over, tracking the particles through the forward shielding and the active parts of the detector. Also in this case, the initial detector layout was assumed. Since the subject of this work is initial detector commissioning, only muons are considered in the following; these particles, if energetic enough, will traverse the forward shielding and leave clean signals in the detectors. The software tools and simulated samples are summarized at [14].

Rates of muons crossing various sub-detectors are given in Table 6. Criteria are applied that ensure that the muons leave enough redundant signals to be useful for calibration or alignment studies. In the MDTs, at least three segments are required, and hits on at least four end-cap

¹The vacuum and optics expected during high-luminosity running have been used in this study because the machine parameters during the commissioning phase were not yet available. A new set of studies has recently been started [13] to evaluate the machine-induced background at IP1 during the machine commissioning period in Spring, 2007.

Detector	Rate (Hz)	Total number of events
MDT (end-cap)	59	1.0×10^8
MDT (barrel)	29	5.2×10^7
TRT	15	2.7×10^7
SCT	29	4.9×10^7
Pixels	0.4	6.7×10^5
EM calorimeter	1.2	2.1×10^6
Tile calorimeter	1.3	2.3×10^6
HEC	0.3	5.3×10^5
FCAL	0.1	1.8×10^5

Table 6: *Beam-halo muon rates in the various sub-detectors (see text for explanations). The total numbers of events assume a two month single-beam period with 30% effective data-taking time.*

wheels or disks are requested in the Inner Detector. The minimal calorimeter energy depositions are 5 GeV in the EM-calorimeters, 20 GeV in the Tilecal and in the HEC, and 50 GeV in the FCAL. Calorimeter energy deposit distributions are displayed in Fig. 11.

Within our assumptions, the expected statistics are clearly promising, particularly in the muon end-cap system where 10^8 tracks are expected assuming a two month single beam period with 30% effective data taking time. For the central detectors, the numbers scale geometrically (the systems with smaller transverse section see proportionally less muons), but are still very significant for the TRT and SCT. These numbers assume nominal magnetic field settings. The study was repeated with all fields switched off and similar results were obtained.

3.4 Beam-gas

During the single-beam period, beam-gas collisions occurring directly inside the ATLAS Inner Detector cavity are also a potentially useful source of data for detector commissioning. The beam-gas simulation depends on the vacuum and beam current, but is otherwise independent of the details of the machine configuration.

Beam-gas collisions were primarily generated as fixed-target proton-proton collisions using the PYTHIA generator [15], which provides the event-by-event details like particle multiplicities and energy distributions, and the basic proton-nucleon cross-section (the inelastic cross-section of a 7 TeV proton on a nucleon at rest, *i.e.* at a centre-of-mass energy of 114.6 GeV, is 47.5 mb). For a given atomic species (of mass number A) present in the cavity, the cross-section can then be written as $\sigma_A = \sigma_p \times A^{0.7}$, and for a molecule one simply sums over the atoms.

According to [11], the main gases present in the LHC vacuum pipe at machine start-up are expected to be H₂, CH₄, CO and CO₂, with residual densities of around 10^{13} molecules/m³ per molecule species at the entrance of the ATLAS cavern. Assuming uniform densities throughout the ATLAS cavity, and as above an initial beam-current equal to 1/200 of the nominal high-luminosity current, the interaction rates listed in Table 7 were obtained for several windows around the interaction point (the rates are given for inelastic collisions). The software tools and simulated samples are summarized at [14].

Inside the Inner Detector acceptance, one expects about 1.7×10^9 charged pions and about 6×10^8 neutral pions with $p_T > 1$ GeV during the single beam period.

These events would be useful, *e.g.*, for Inner Detector alignment purposes since they resemble p-p interactions. However, it looks difficult to trigger on these events, which are essentially boosted minimum-bias, using the standard triggers since the transverse energy of the outgoing

Window (z)	Rate (kHz)	Total numbers of events
± 23 m	60	1.1×10^{11}
± 3.5 m	9	1.7×10^{10}
± 20 cm	0.6	1.0×10^9

Table 7: *Inelastic beam-gas collision rates integrated over the whole ATLAS cavity (± 23 m), over the Inner Detector acceptance (± 3.5 m) and close to the nominal interaction point (± 20 cm). The total numbers of events assume a two month single beam period with 30% data taking time.*

particles is very small (see Fig. 12). This and related issues are discussed in the next section.

4 Trigger issues

We report here preliminary thoughts on how to trigger on the “physics” events discussed in the previous sections.

4.1 Standard ATLAS triggers

The most obvious method is to use RPCs to trigger on cosmic muons and TGCs to trigger on beam-halo muons. The timing could be given by a free-running 40 MHz clock, although for beam-halo muons some correlation with the machine clock may be available.

Preliminary full-simulation studies [16] of the LVL1 muon trigger as it is, without relaxing, for example, the projectivity requirements toward the interaction centre, indicate that about 100 Hz of cosmic muons pass the LVL1 RPC low- p_T trigger and about 1 Hz of beam-halo muons pass the LVL1 TGC low- p_T trigger. Figure 13 shows the distribution of cosmic muons triggered by the RPC in the $\eta - \phi$ plane. The flux is maximum on the top and bottom of the detector and vanishes on the horizontal plane, as expected. These rates are low enough not to represent a worrying background during normal data taking at the LHC, and large enough to give potentially useful samples during the commissioning phase. For instance, using the standard LVL1 RPC trigger, and assuming a data taking efficiency of 50%, one should be able to collect more than 10^8 cosmic events in three months. In addition, these muons are those which best mimic tracks from the pp collisions, since by definition they pass close to the interaction centre.

The above rates can most likely be increased during the commissioning phase by relaxing or adjusting some of the LVL1 trigger requirements. Indeed, there is a lot of flexibility built in the muon trigger system, where most of the settings and parameters are programmable. For instance, it should be possible to adjust the timing of the RPC signals in the Coincidence Matrix to cope with down-going muons, it should be possible to open the LVL1 roads (this will be limited mainly by cabling constraints), it should be possible to relax the 3/4 majority request on the number of hit layers, it should be possible to use only one projection in the Coincidence Matrix, etc. These possibilities are under investigation. Similar considerations apply to the TGC-based trigger for beam-halo muons, although the flexibility in the end-caps is more limited.

Another issue presently under study is the implementation of a cosmic muon trigger based on Tilecal [17]. This would allow the calorimeters to take cosmic runs as early as 2004-2005, i.e. before the RPC system will become available at the end of 2005, and relies on the excellent signal-to-noise ratio for muons in Tilecal ($S/N \sim 5$ (40) with LVL1 electronics (optimal filtering)). Preliminary studies for the barrel part have considered a scheme based on the coincidence of pairs of back-to-back (in η/ϕ) trigger towers². Asking an energy deposition of at least 1.5 GeV

²Trigger towers have a granularity of $\Delta\eta \times \Delta\phi = 0.1 \times 0.1$ and extend over the full Tilecal depth.

in both towers of a pair, and using 16 top and 16 bottom Tilecal azimuthal modules, would give a trigger rate of ~ 130 muons per hour. This method will allow Tilecal to self-trigger, as well as to provide a trigger to the liquid-argon EM calorimeter.

4.2 Dedicated scintillator detectors

Triggering on beam-gas interactions, which are potentially very useful data for commissioning the Inner Detector, is a more difficult question, because of the soft p_T spectrum of the produced particles. A trigger based on the energy deposition in the forward calorimeter doesn't look promising at a first sight. For instance, requiring a total energy of 15 GeV in one of the FCAL would select ~ 10 Hz of beam-gas events. This threshold has to be compared with an electronic noise of order 10 GeV.

The only solution today seems to be the use of dedicated devices, like the recently-proposed scintillator detectors to be installed inside the ATLAS inner cavity in front of the end-cap cryostats, at a distance $z \simeq \pm 3.5$ m from the interaction centre (see Fig. 14). These detectors would replace part of the JM moderator. They will most likely cover the radial region $14 < R < 100$ cm (corresponding to $1.9 < |\eta| < 3.9$) and have a readout segmentation into eight ϕ -sectors and two η -sections. They could be read out by photomultipliers originally belonging to the crack scintillators inserted between the barrel and end-cap cryostats and temporarily diverted from their primary goal. These detectors would be extremely useful to trigger not only on beam-gas events, but also on beam-halo muons incident at radii below ~ 2 m (which corresponds to the lower edge of the TGCs) and on minimum-bias events during the first collisions.

Preliminary studies have been performed with scintillator planes in the above configuration, and for the three categories of events listed above (beam-halo muons at low radius, beam-gas events occurring inside the ATLAS cavity, and head-on minimum bias events). The resulting performance is summarized in Fig. 15 and described in the following. The analysis criteria are quite simple and can certainly be improved, implying that these results are a conservative estimate.

The efficiency for beam-halo muons is given in the top panel of Fig. 15 for exactly one hit on either one or both scintillator planes, as a function of the muon radius at cavern entrance. The two-plane efficiency peaks at 40%, and is above 10% over most of the Inner Detector radial acceptance. The inefficiencies come from low energy muons stopped in the ATLAS forward shielding, and from the strict request of only one hit on each plane (additional hits are caused by secondaries accompanying the muons and can occur frequently). A non-zero efficiency is also found for muons entering the cavern at a radius beyond the scintillator acceptance, and in this case the one-plane efficiency dominates. These triggers are caused by secondaries coming from muons actually crossing the barrel calorimeters. Folding these numbers with the radial distribution shown in Fig. 10 gives a total trigger rate of about 50 Hz.

The efficiencies for beam-gas and beam-beam events are displayed in the middle and lower panels of Fig. 15, as a function of the inner radius (denoted R_{\min} on the plots) of the scintillator planes, and for various total multiplicity cuts. The beam-gas efficiency is averaged over $|z| \leq 3.5$ m, assuming a uniform vertex distribution over this range. Requiring at least one hit in the full detector ($R_{\min} = 14$ cm) gives an efficiency of around 70% in both cases, where the lost 30% is mainly due to elastic and diffractive events. Requiring at least 10 hits reduces the beam-gas efficiency to 50% with practically no impact on the beam-beam efficiency. The R_{\min} dependence allows us to estimate the efficiency when only the outer η segment of the scintillators is used (*e.g.* if the inner segment is damaged by radiation), as a function of the radius of the transition between the inner and outer segments.

5 Ongoing studies and future plans

As soon as the rates for cosmic muons, beam-halo muons and beam-gas events reported in the previous sections were obtained, studies started in the various sub-detector and trigger performance groups to understand the utility of these events for, *e.g.*, timing, alignment and calibration purposes during the commissioning period. A few examples are mentioned here.

Cosmic and halo muons are long lever arm tracks that should allow adjustments of the sub-detector relative timing across the whole detector. Beam-halo and beam-gas events are expected in time with the beam, and will thus allow adjustments between the ATLAS and LHC clocks. It should thus be possible to start p-p data taking with system clocks already synchronized [18].

Preliminary studies of the barrel EM calorimeter, based on the cosmic rates reported in Section 3.1, indicate that using cosmic muons the position of the calorimeter relative to the Inner Detector could be measured to ~ 0.5 mm, the calorimeter timing to ~ 1 nsec and the calorimeter uniformity to $\sim 0.5\%$ [19]. Similar studies have started also in the Inner Detector [20], Tile Calorimeter [21], Hadronic End-cap and Forward Calorimeter [22] and Muon Detectors [23]. Software tools and reconstruction algorithms optimized for these atypical events are also being investigated.

The proposed scintillator trigger would allow events leaving signals at low radius to be recorded, like beam-gas events and beam-halo muons. This would then enable specific studies (*e.g.* timing and alignment) of the end-cap calorimeters and trackers. It should also be noted that highly non-projective tracks (like the nearly horizontal halo muons) do have a specific interest in that they couple detector elements that do not lie on tracks originating from the interaction point, and therefore provide additional redundancy in calibration studies.

6 Conclusions

The event rates expected in ATLAS from cosmic ray muons, and from beam-halo muons and beam-gas collisions during the LHC single-beam period, have been estimated with full simulation studies. In all cases, rates were found to be significant and useful for commissioning the ATLAS detector before the first p-p collisions. Preliminary studies of the individual sub-detectors and of the trigger system have shown promising potential of these events for alignment, calibration and timing studies.

Tools, documents and summary of Monte Carlo samples for detector commissioning with physics data are summarized at [24], including details of the cosmic [9] and beam-halo and beam-gas [14] studies.

7 Acknowledgments

We would like to thank Vadim Talanov for his work on the machine background simulation at IP1. We profitted from many useful discussions with Nick Ellis, Per Grafstrom, Richard Hawkings, Alejandro Nisati and Stefano Veneziano during these studies.

References

- [1] See for instance P. Collier, “Machine commissioning: first beams to first collisions”, in Proceedings of the XII Chamonix Workshop, 2003, <http://ab-div.web.cern.ch/ab-div/Conferences/Chamonix/chamx2003/contents.html>.
- [2] <http://agenda.cern.ch/fullAgenda.php?ida=a031081#s12>.

- [3] <http://agenda.cern.ch/fullAgenda.php?ida=a03190#s2>.
- [4] <http://agenda.cern.ch/displayLevel.php?fid=164>.
- [5] Radiation Background Task Force,
http://atlas.web.cern.ch/Atlas/GROUPS/PHYSICS/RADIATION/RadiationTF_document.html
- [6] Formula (23.5) in the “Review of Particle Properties”, K.Hagiwara *et al.*, Phys. Rev. **D66** (2002).
- [7] A. Dar, Phys. Rev. Lett. **51**, 227 (1983).
- [8] See comments in Section 23.3.1 in the 2002 “Review of Particle Properties”, K.Hagiwara *et al.*, Phys. Rev. **D66** (2002).
- [9] <http://rmcphers.home.cern.ch/rmcphers/atlas/cosmics/>.
- [10] I. Azhgirey, I. Baishev, K.M. Potter and V. Talanov, LHC Project Note 324 and LHC Project Report 567.
- [11] A. Rossi and N. Hilleret, LHC Project Report 674 (2003).
- [12] P. Collier, private communication.
- [13] Work done by V. Talanov and collaborators.
- [14] http://boonekam.home.cern.ch/boonekam/beam_halo.htm.
- [15] T. Sjöstrand, Comp. Phys. Comm. **135** 238-259 (2001).
- [16] ATLAS First-level trigger TDR, CERN/LHCC/98-14.
- [17] See for instance R. Teuscher, talk given at the Physics Commissioning meeting, July 16 2003, <http://agenda.cern.ch/fullAgenda.php?ida=a032115>.
- [18] See “Commissioning the LVL1 Trigger System”, Nick Ellis at the ATLAS Commissioning workshop, 14 September 2003, Prague, <http://agenda.cern.ch/age?a03190>.
- [19] See “Commissioning ECAL with cosmic muons”, Fabiola Gianotti at the ATLAS Commissioning workshop, 14 September 2003, Prague, <http://agenda.cern.ch/age?a03190>.
- [20] See “Commissioning with physics data, Inner Detector Plans”, Markus Elsing at the ATLAS Commissioning workshop, 14 September 2003, Prague, <http://agenda.cern.ch/age?a03190>.
- [21] See “Commissioning TileCal with Cosmic Ray Muons”, Richard Teuscher at the ATLAS Commissioning workshop, 14 September 2003, Prague, <http://agenda.cern.ch/age?a03190>.
- [22] See “HEC and FCAL: commissioning with muons?”, Rob McPherson at the ATLAS Commissioning workshop, 14 September 2003, Prague, <http://agenda.cern.ch/age?a03190>.
- [23] See “Muon System Commissioning”, Claude Guyot and Jim Shank at the ATLAS Commissioning workshop, 14 September 2003, Prague, <http://agenda.cern.ch/age?a03190>.
- [24] <http://polesell.web.cern.ch/polesell/commissioning.html>.

Commissioning in different phases

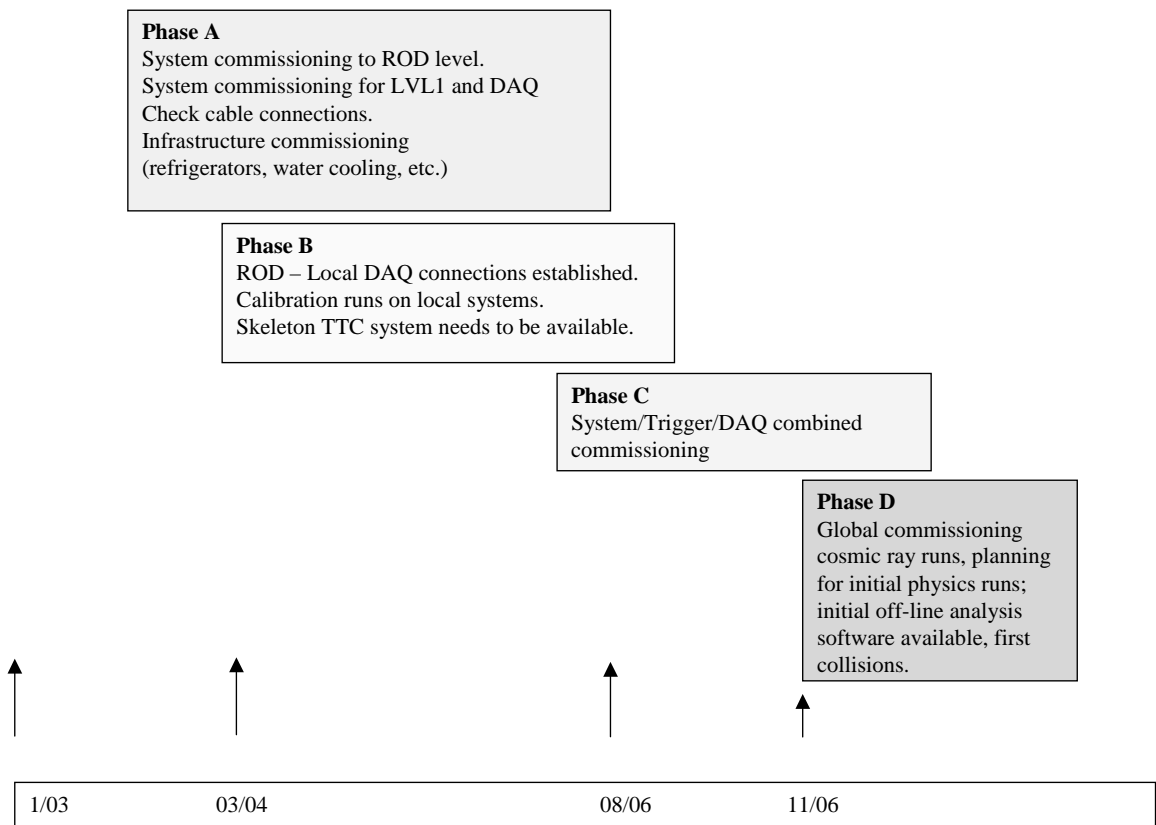


Figure 1: Sketch of the ATLAS commissioning plan as seen by Technical Coordination.

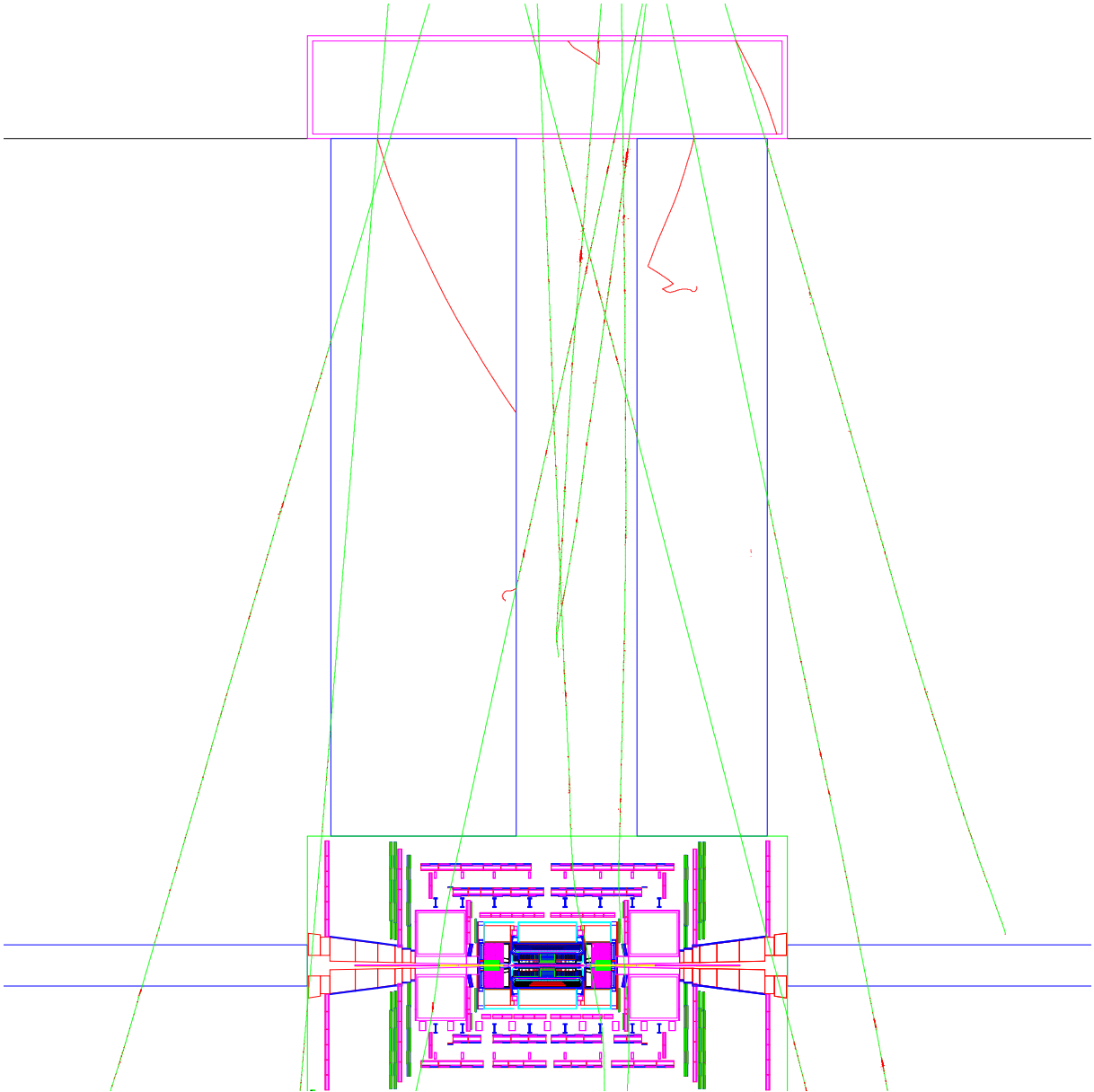


Figure 2: Layout of the ATLAS experimental hall, access shafts and surface buildings as described in the GEANT3 simulations used for this study.

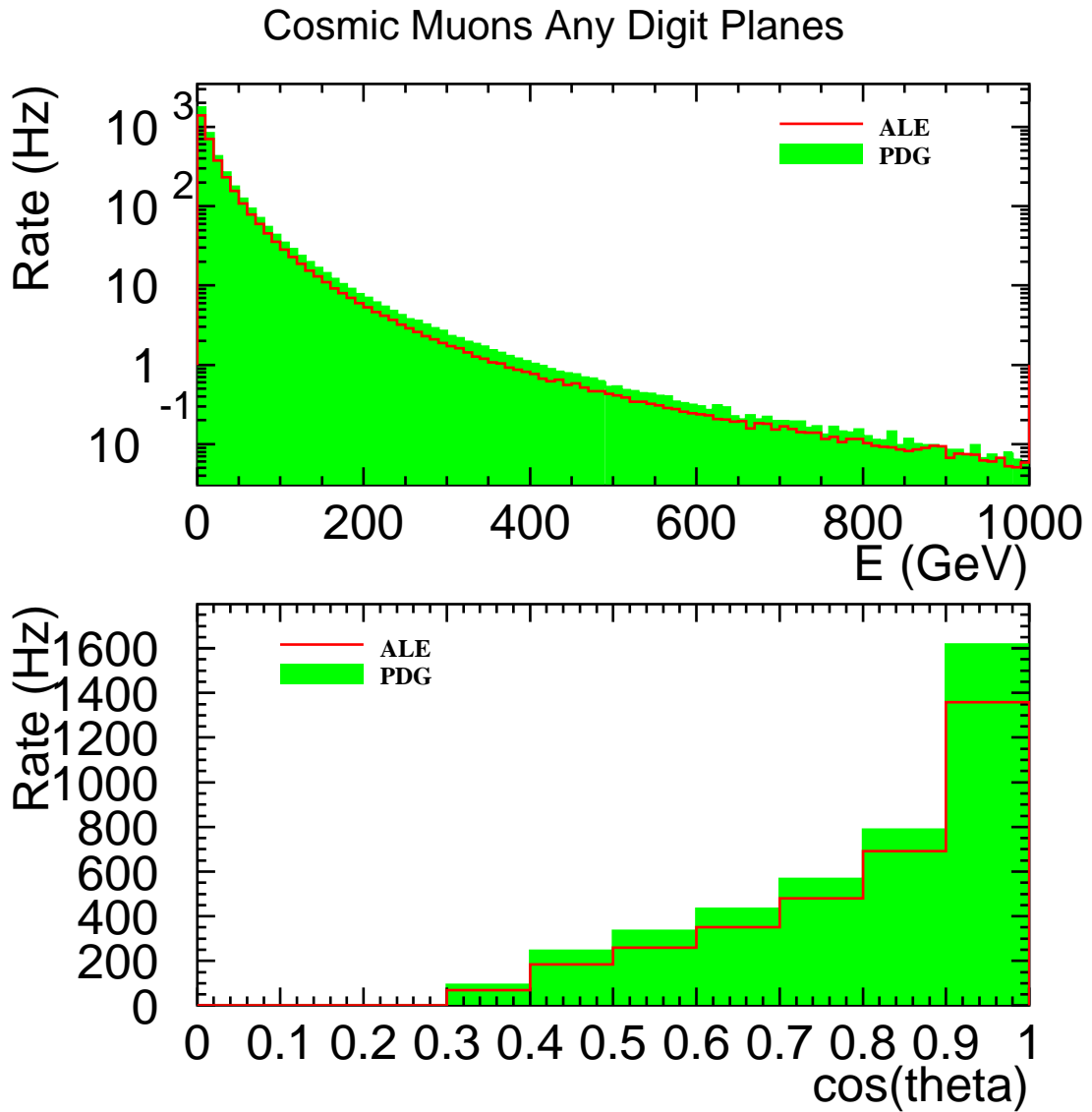


Figure 3: Energy and azimuthal angle distributions of cosmic ray muons with at least one detector hit predicted by these studies. The quantities are defined as the muons enter the standard ATLAS GEANT3 detector volume. The ALE and PDG generators are described in Section 3.1.

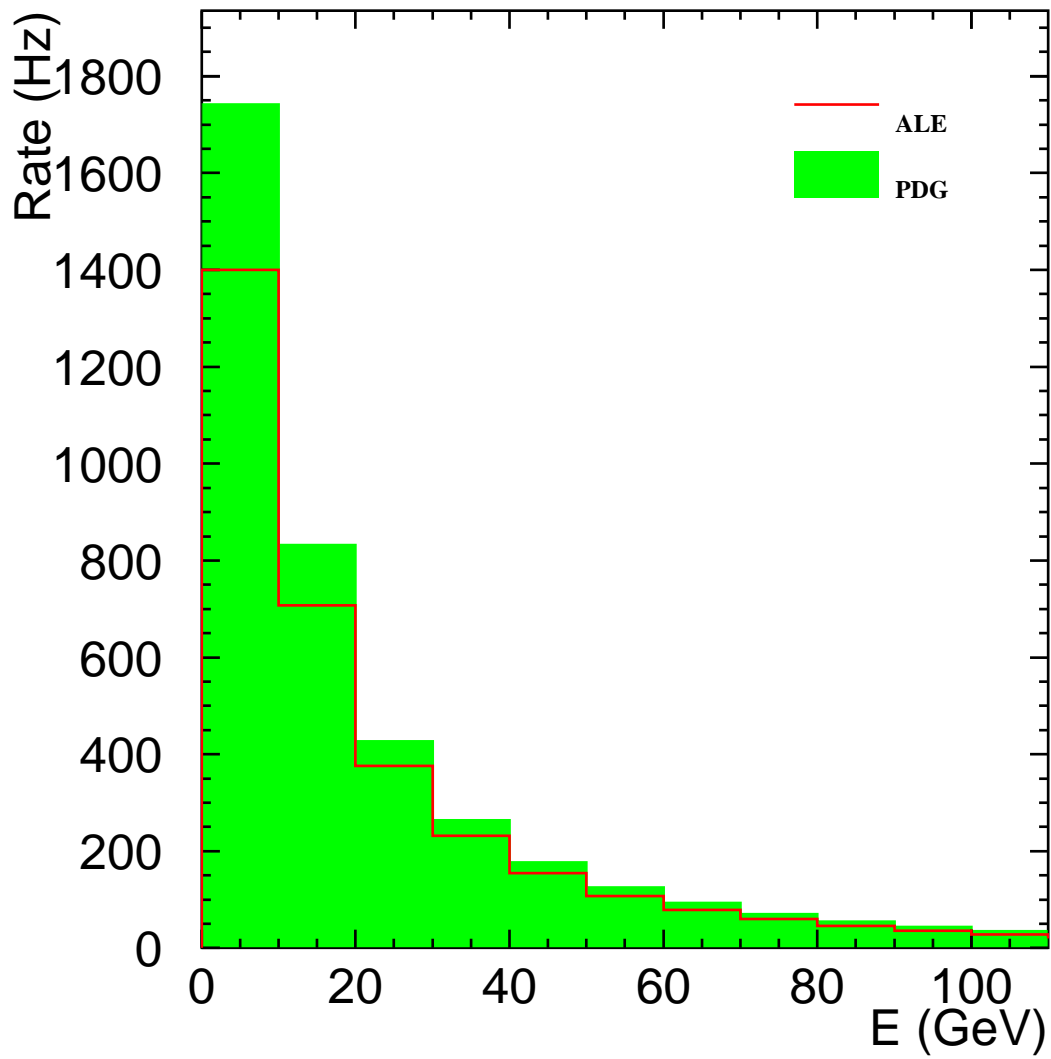


Figure 4: Same as the energy plot in Fig. 3, with the low energy region expanded. The ALE generator is expected to give more reliable results, particularly for low energy muons.

Cosmic Muons, RPC Top+Bot + PIX Digit Planes

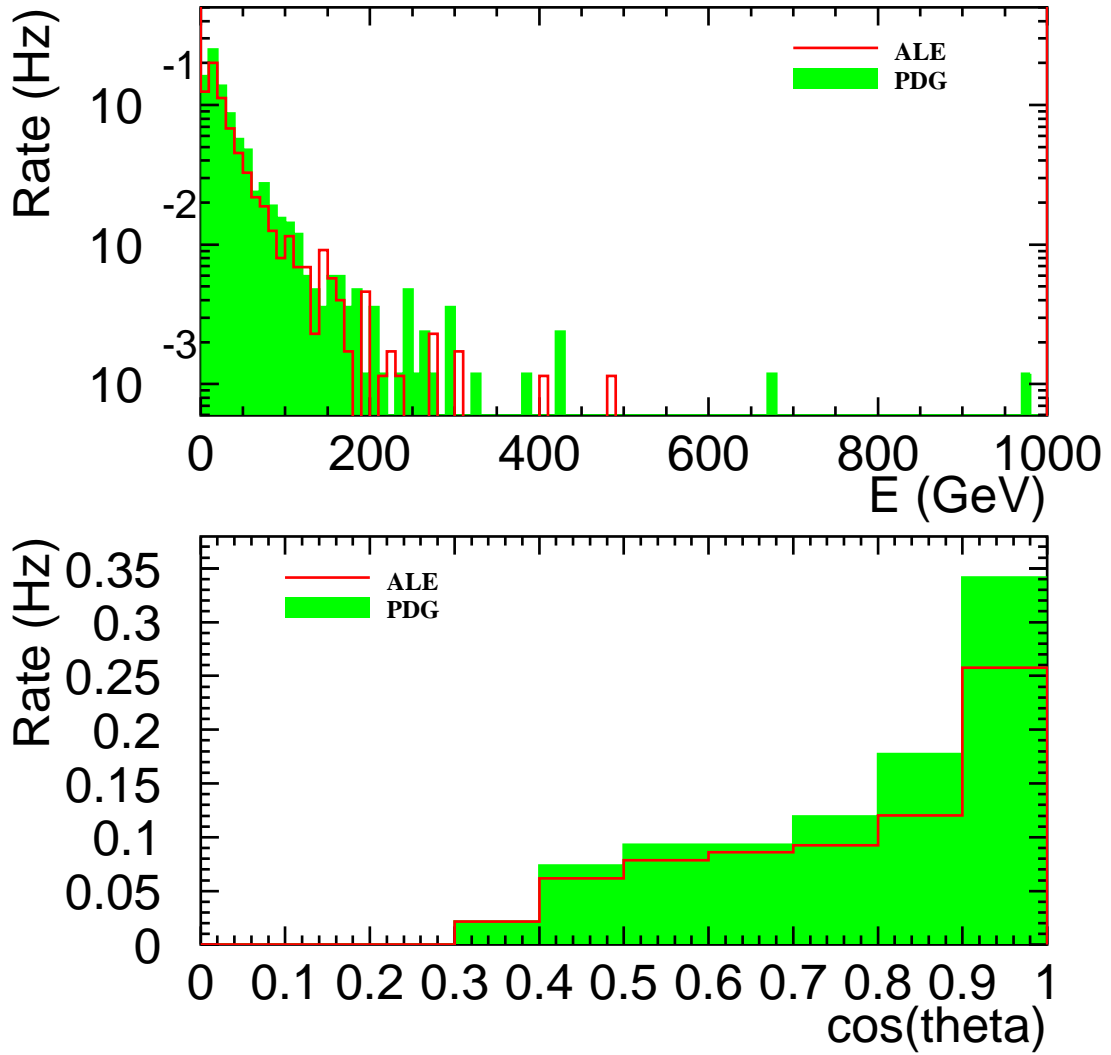


Figure 5: Energy and azimuthal angle distributions of cosmic ray muons with at least one pixel detector hit predicted by these studies. The events are also required to have muon trigger chamber hits on both the upper ($Y > 0$) and lower ($Y < 0$) halves of ATLAS. The quantities are defined as the muons enter the standard ATLAS GEANT3 detector volume.

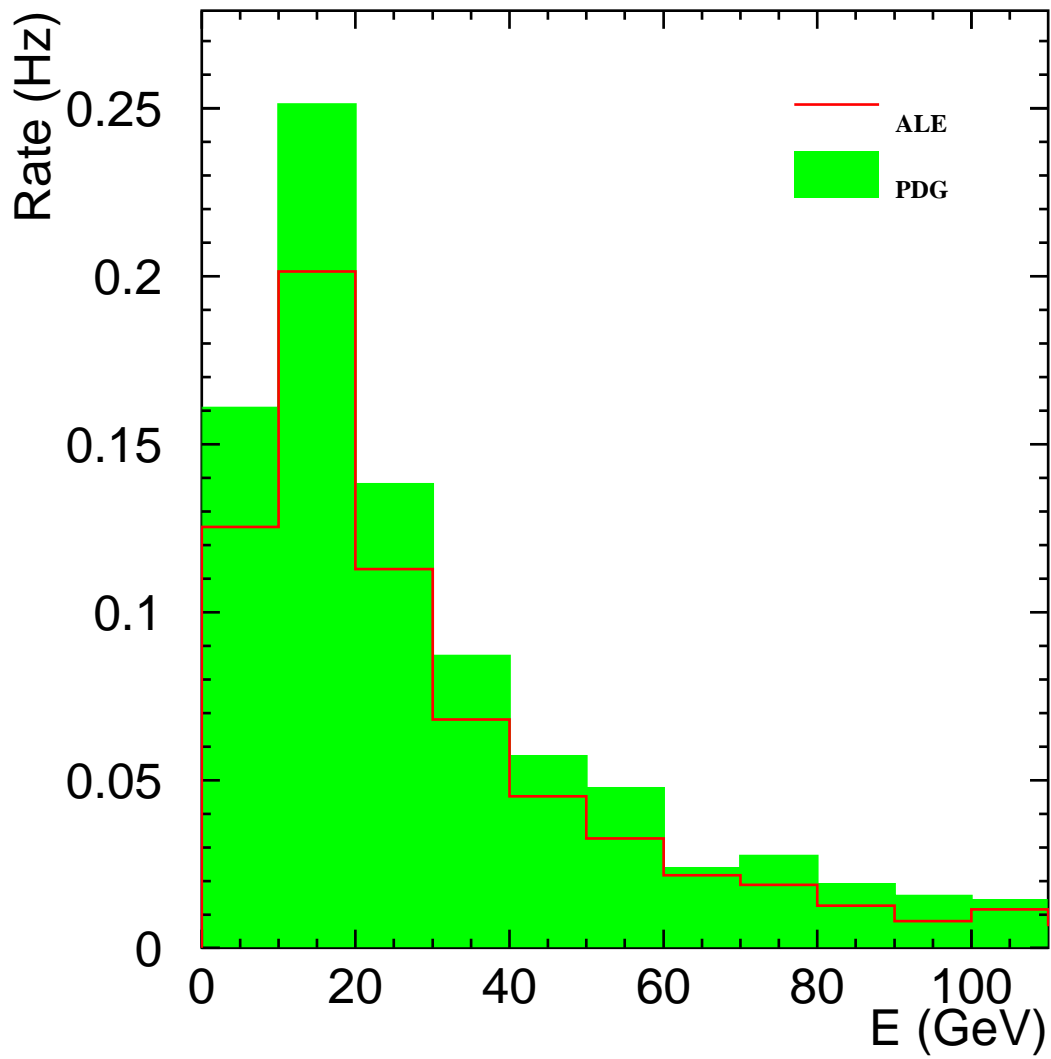


Figure 6: Same as the energy plot in Fig. 5, with the low energy region expanded. The ALE generator is expected to give more reliable results, particularly for low energy muons.

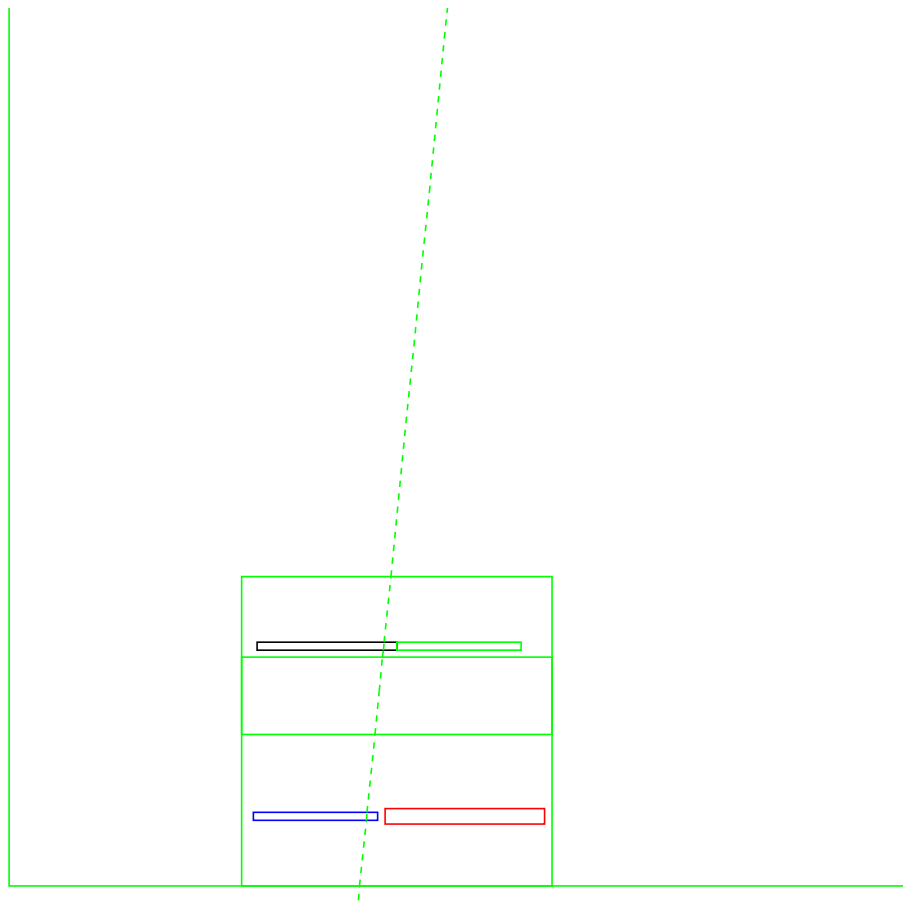


Figure 7: Layout of the muon telescope used to measure muon fluxes in the ATLAS experimental hall, as described in GEANT3.

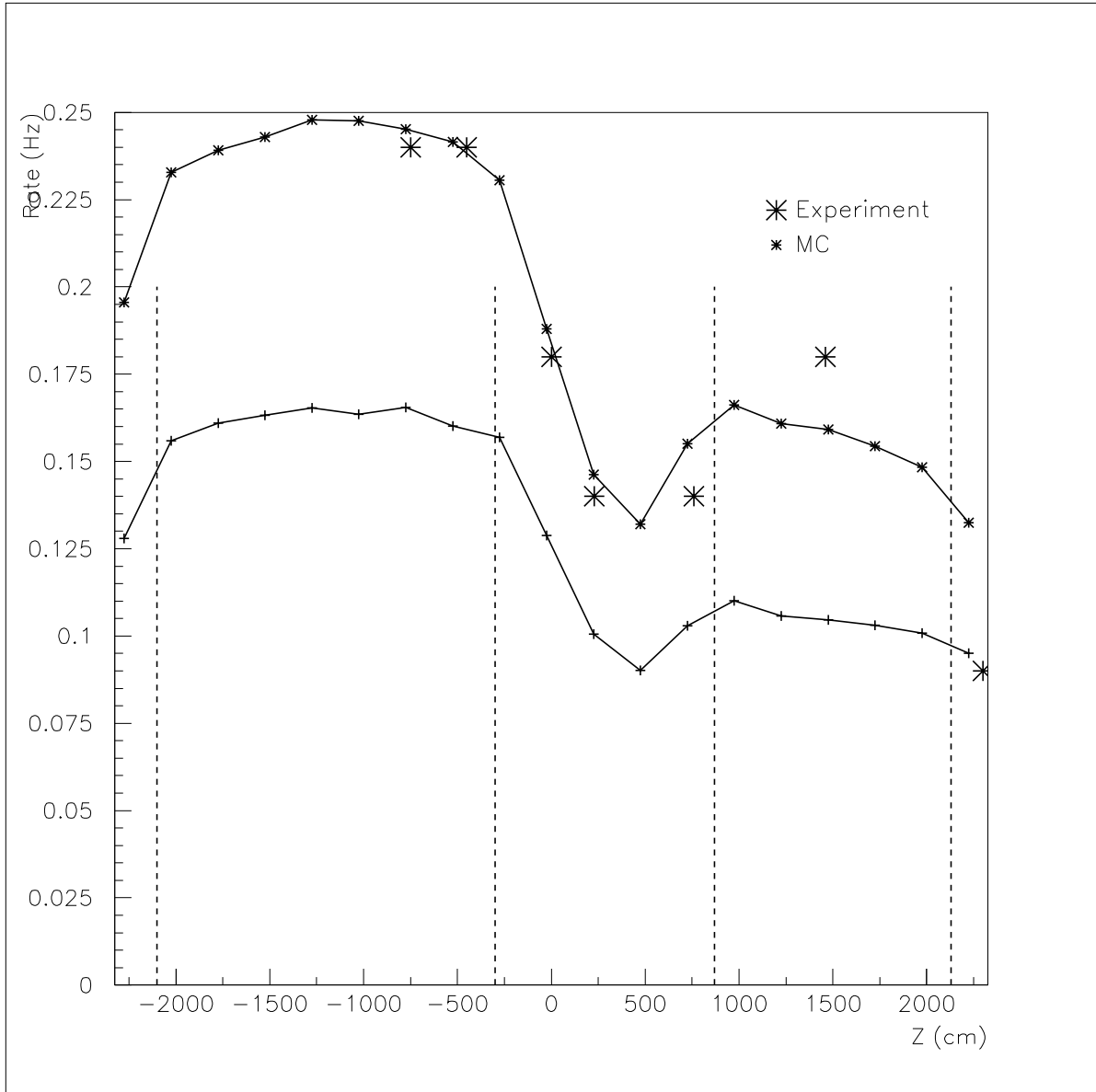


Figure 8: Measured muon vertical fluxes compared to simulation predictions. The upper curve (and nearby measurements) corresponds to simulations performed along the central axis of the ATLAS cavern, while the lower curve (along with one measurement near $Z=2000$ cm) is for simulations of the flux at the cavern wall.

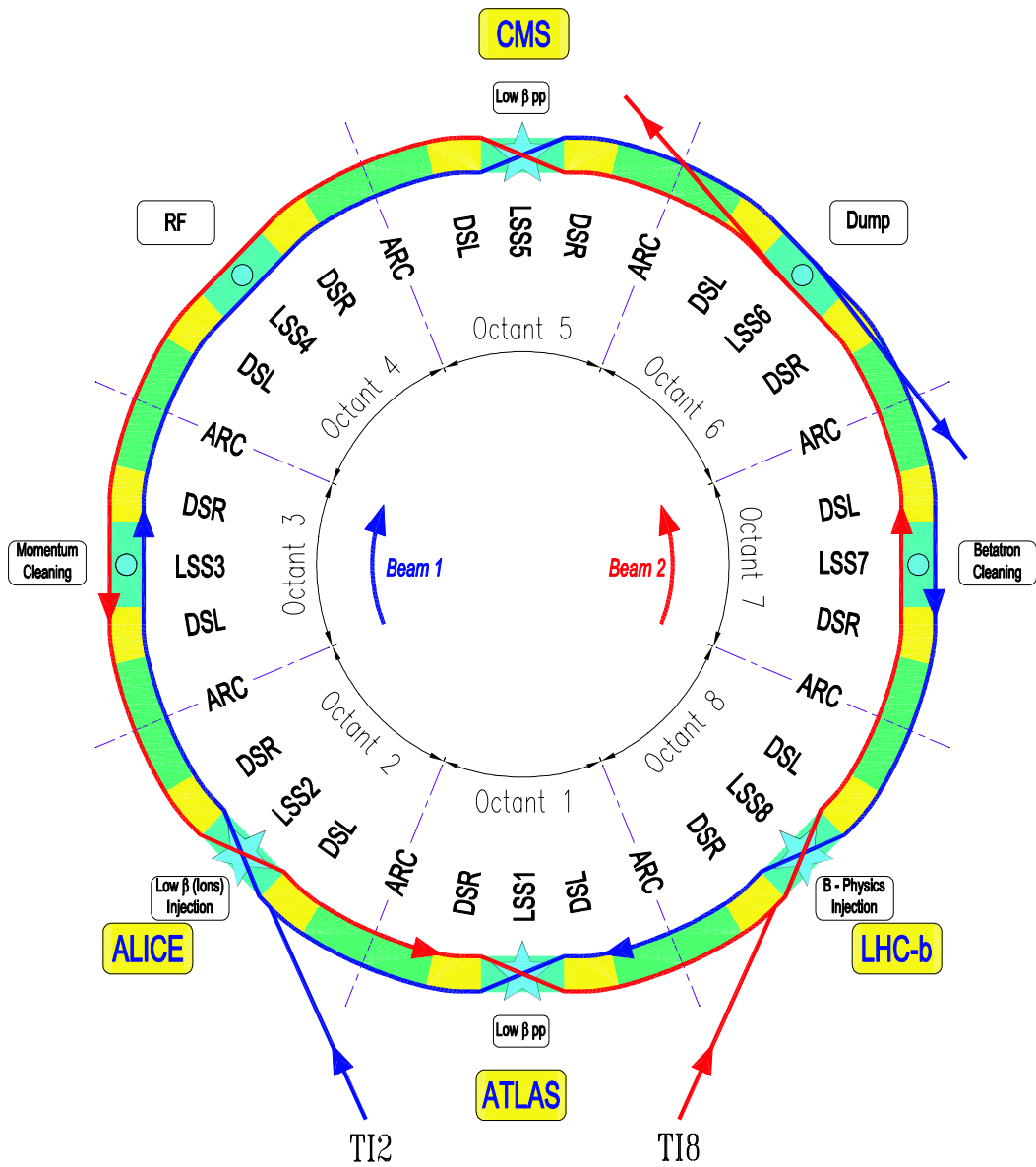


Figure 9: Schematic layout of the LHC ring.

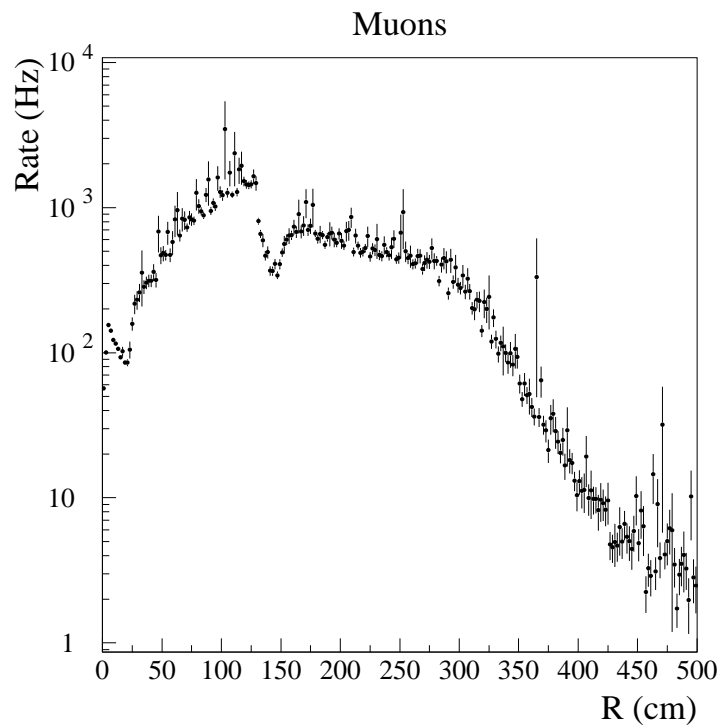
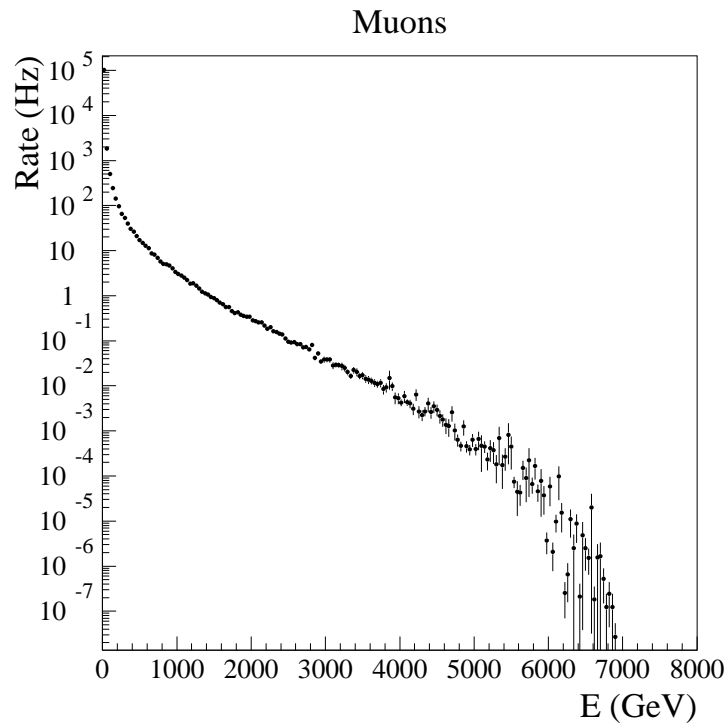


Figure 10: Energy distribution (top) and radial distribution (bottom) of beam-halo muons entering the ATLAS cavern.

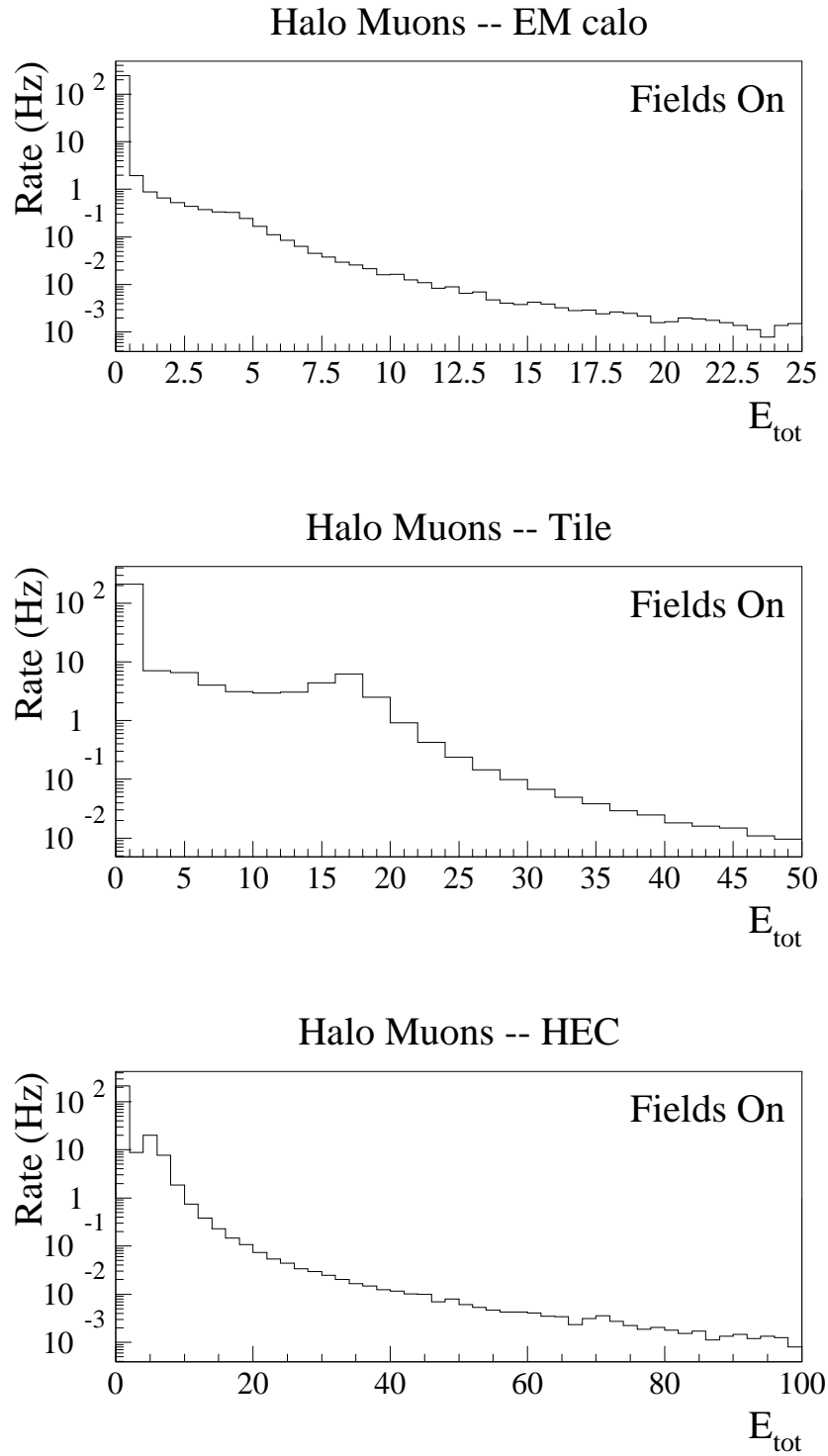


Figure 11: Total energy deposition in the EM calorimeter (top), in the Tile calorimeter (middle), and in the HEC (bottom) from beam-halo muons.

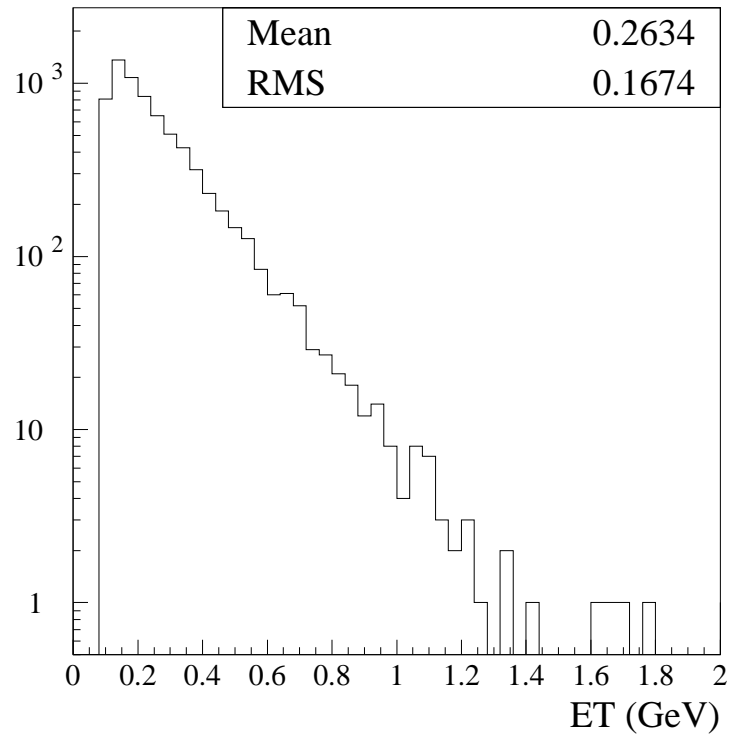
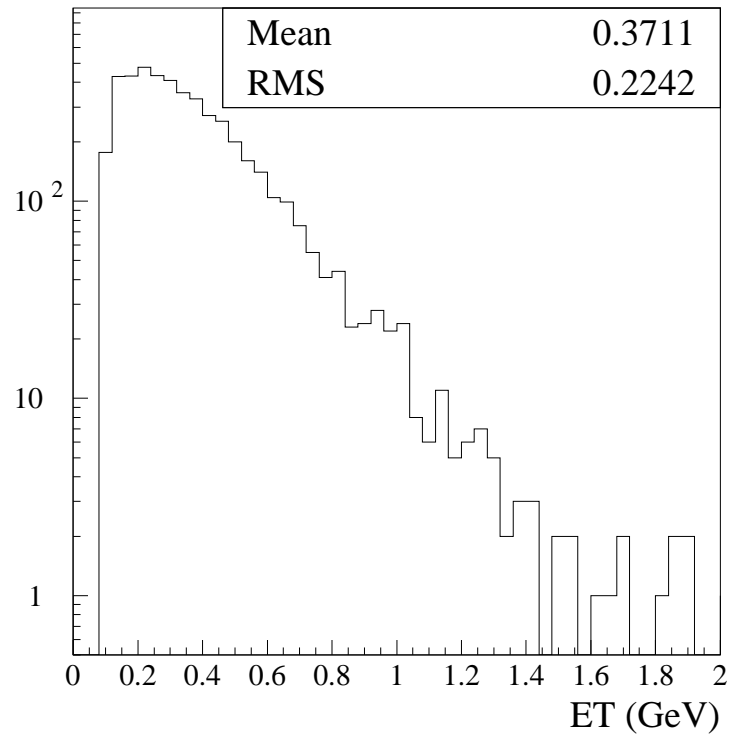


Figure 12: The transverse energy spectrum of particles produced in beam-gas events. The upper plot is for charged particles, and the lower plot is for neutrals.

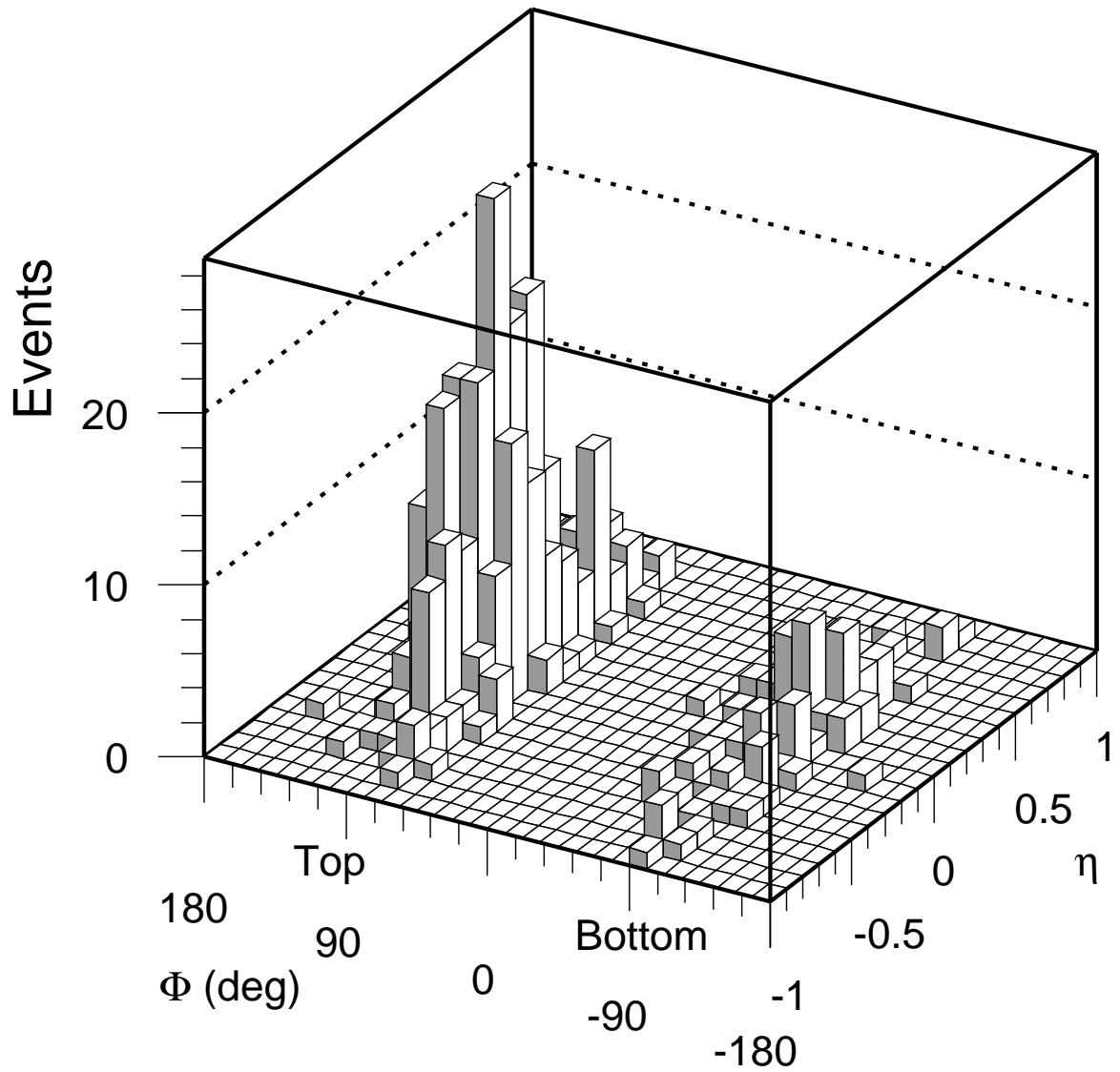


Figure 13: Distribution in the $\eta - \phi$ plane of cosmic muons triggered by the standard LVL1 low- p_T muon trigger [16].

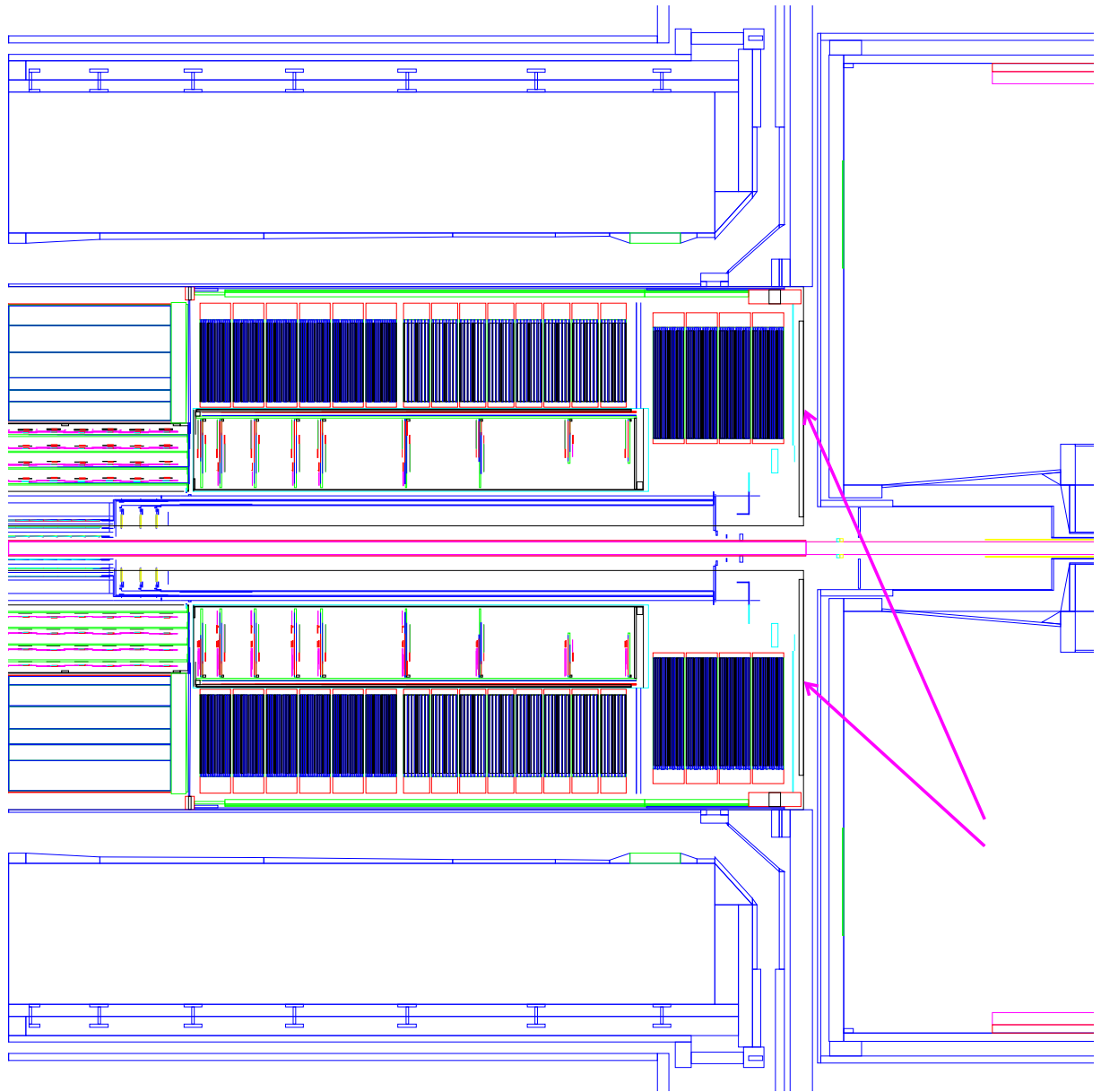


Figure 14: Schematic longitudinal view of half of the inner cavity, showing the location of the JM moderator where the recently-proposed scintillator devices should be installed.

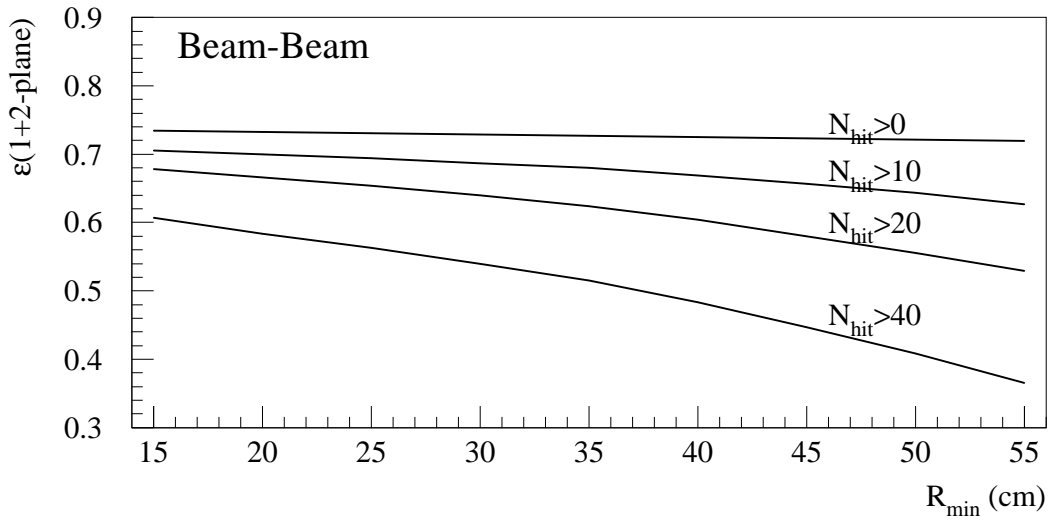
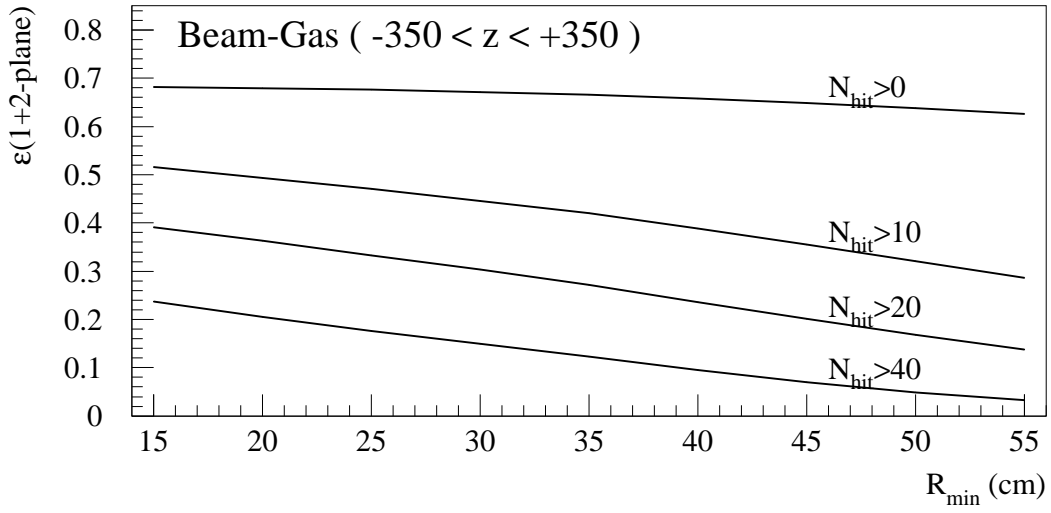
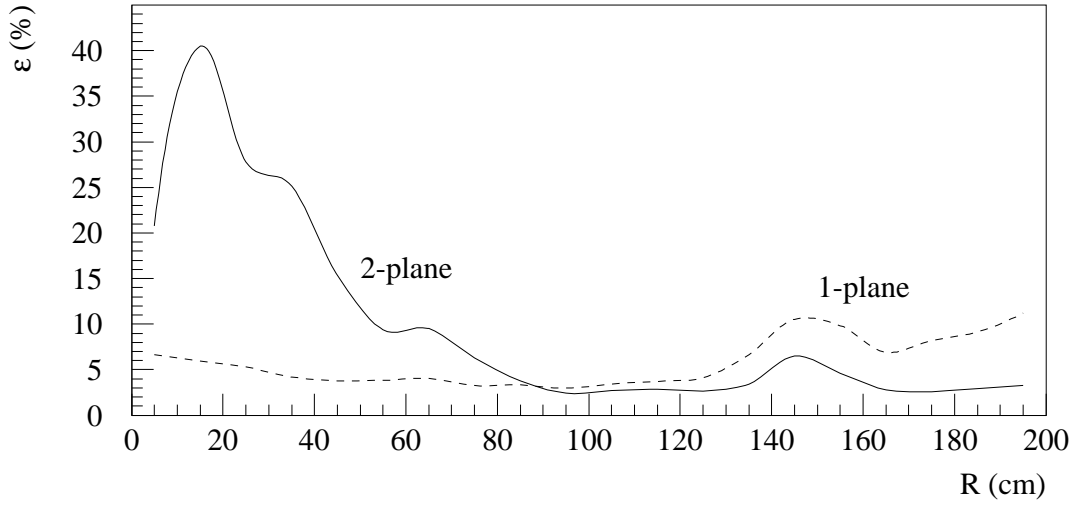


Figure 15: Efficiency for exactly one hit on either or both trigger scintillators for beam-halo muons as a function of the radius of the muon entering the cavern (top); the efficiencies for beam-gas (middle) and beam-beam (bottom) events as a function of the inner radius of the scintillator planes. See Section 4 for detailed discussion.